

# Deepfake Caricatures: Amplifying attention to artifacts increases deepfake detection by humans and machines

Camilo Fosco\*

MIT

camilolu@mit.edu

Emilie Josephs\*

MIT

ejosephs@mit.edu

Alex Andonian

MIT

andonian@mit.edu

Allen Lee

MIT

allenlee@mit.edu

Xi Wang

MIT

nicole.xiwang@gmail.com

Aude Oliva

MIT

oliva@mit.edu

## Abstract

Deepfakes pose a serious threat to digital well-being by fueling misinformation. As deepfakes get harder to recognize with the naked eye, human users become increasingly reliant on deepfake detection models to decide if a video is real or fake. Currently, models yield a prediction for a video’s authenticity, but do not integrate a method for alerting a human user. We introduce a framework for amplifying artifacts in deepfake videos to make them more detectable by people. We propose a novel, semi-supervised Artifact Attention module, which is trained on human responses to create attention maps that highlight video artifacts. These maps make two contributions. First, they improve the performance of our deepfake detection classifier. Second, they allow us to generate novel “Deepfake Caricatures”: transformations of the deepfake that exacerbate artifacts to improve human detection. In a user study, we demonstrate that Caricatures greatly increase human detection, across video presentation times and user engagement levels. Overall, we demonstrate the success of a human-centered approach to designing deepfake mitigation methods.

## 1. Introduction

Fake or manipulated video media (“deepfakes”) pose a clear threat to the integrity of online spaces that rely on video, from social media, to news media, to video conferencing platforms. To the human eye, these computer-generated fake videos are increasingly indistinguishable from genuine videos [38, 17]. Computer vision models, however, can achieve impressive success at deepfake detection. Thus, the future of deepfake detection for humans may become a problem of AI-assisted decision-making, where humans must incorporate the output of a machine learning

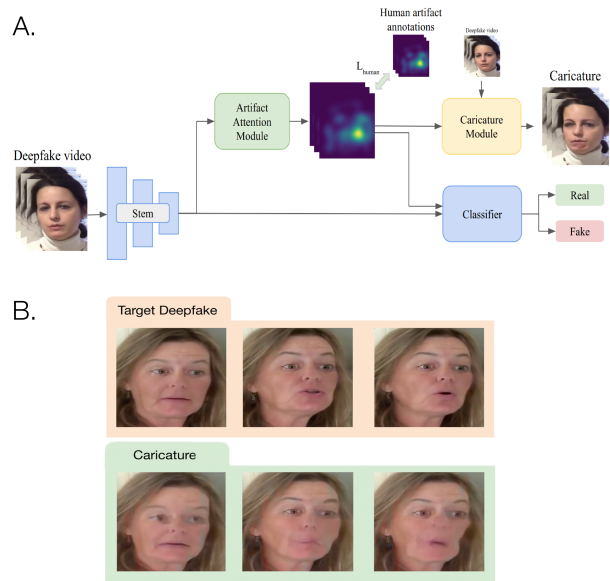


Figure 1. A. Overview of our framework. The model learns to identify artifacts visible to humans, then amplify them to generate Deepfake Caricatures: transformations of the original videos where artifacts are more visible. B. Example frames of a standard deepfake video (top) and a deepfake caricature (bottom).

model into their judgment process.

Previous work on AI-assisted decision making indicates that the design and format of a decision aid strongly determines whether it will impact human behavior [52, 49, 13, 22, 4]. In the domain of deepfake signaling, traditional methods of flagging manipulated video have relied on text-based prompts. However, recent studies indicate relatively low rates of compliance when the model’s prediction is conveyed using text: in one study, participants shown model predictions via text updated their response only 24% of the

time, and switched their response (from "real" to "fake", or vice versa) only 12% of the time [17]. More innovative approaches have been proposed, such as showing users a heatmap of regions predicted to be manipulated [8], but this did not increase acceptance rates relative to text-based indicators. Overall, to make an impact, the development of deepfake detection models must proceed alongside the exploration of innovative and effective ways to alert human users to a video's authenticity.

We present a novel framework that provides strong classical deepfake detection, but crucially also creates a compelling visual indicator for fake videos by amplifying artifacts, making them more detectable to human observers. Because humans tend to be highly sensitive to distortions in faces, we hypothesize that focusing our visual indicator on amplifying artifacts is likely to yield a highly detectable and compelling visual indicator. Our model, "CariNet", identifies key artifacts in deepfakes using a novel *Artifact Attention Module*, which leverages both human supervision and machine supervision to learn what distortions are most relevant to humans. CariNet then generates **deepfake caricatures**, distorted versions of deepfakes, using a *Caricature Generation Module* that magnifies unnatural movements in videos, making them more visible to human users.

We make two primary contributions:

- We develop a framework for identifying video artifacts that are relevant to humans. Allowing our deepfake detector to leverage this information boosts its accuracy by more than 5%, showing that human supervision can improve deepfake detection models.
- We generate deepfake caricatures, and show in a user study that they increase human deepfake detection accuracy by up to 40% compared to non-signalled deepfakes.

## 2. Related work

### 2.1. Deepfake detection systems

Deepfake detection is a young but active field. Many novel architectures have been proposed in the last few years to detect videos or images where faces have been digitally manipulated [3, 5, 37, 41, 18, 35].

Some approaches detect fake faces based on image artifacts in the video frames, such as unnatural amplitude spectra [16], warping artifacts [28, 53], color inconsistencies [23], or blending artifacts [26]. Others detect anomalous biological signals, such as blood volume changes [12], blinking [27], or eye color and specularities [32]. Recently, models have been augmented with attention mechanisms that highlight specific parts of the input, such as face regions (nose, eyes, etc.) [47], the blending boundary between real and

false video [26], or regions that are likely to have been manipulated [24, 44]. Overall, we build on this previous work to develop a novel network that uses attention mechanisms to detect human-relevant artifacts, and amplifies them to increase human detection.

### 2.2. Human face perception

Humans are exceptionally sensitive to the proportions of faces. Psychology research has shown that faces are encoded in memory based on their deviations from a generic averaged face [7, 43], and that the proportions of facial features are at least as important as the particular shape of a facial component for distinguishing among faces [7]. This sensitivity is leveraged in the art style known as "caricature", where distinctive features of a face are exaggerated in a way that makes them easier to recognize and remember [7, 33, 43, 50], by drawing attention to the facial regions that differ most from the norm. Inspired by these caricatures, our method makes distortions of proportions in fake videos more visible, increasing a viewer's ability to recognize the video as fake.

### 2.3. AI-assisted decision making

AI decision aids are increasingly being employed for applications like medical image reading, recidivism prediction, risk assessment, ecological identification, and more [51, 52, 49]. These function by supplementing the judgments of a human user with the output of a machine learning algorithm. Such decision aids improve the accuracy of human decisions, particularly in cases where the AI can detect signals that are complementary to those that humans can detect [49]. However, the design of the communication interface between the model and human user is crucial for human acceptance of the model result. Models that present irrelevant results, are insufficiently transparent to users, or present overly dense outputs are more likely to be disregarded [49, 13, 22, 4]. We hypothesize that amplifying artifacts in deepfake videos is well-suited for improving human deepfake detection: it targets and amplifies the same information humans would use to make an unassisted judgment, in an easy-to-understand format, without adding irrelevant information.

## 3. Model specification

We present a framework that leverages human annotations to detect and amplify video artifacts in deepfakes, using a combination of self attention and human-guided attention maps. Our model, dubbed *CariNet*, contains three main modules (Figure 1)

- An **Artifact Attention Module** that outputs heatmaps indicating the probable location of artifacts in each input frame.

- A **Classifier Module**, consisting of a set of ResNet blocks with self-attention, which estimates whether the video is fake. This module incorporates the output of the artifact attention module to modulate attention toward artifacts.
- A **Caricature Generation Module**, which uses the Artifact Attention maps to amplify artifacts directly in the videos, yielding *deepfake caricatures*.

### 3.1. Artifact Attention module

This module (Figure 2) guides the model towards informative regions in the videos. It consists of an encoder-decoder architecture that reconstructs human annotations. We incorporate human annotations for two reasons: 1) it biases the model toward the artifacts that are informative to humans, and 2) it guides the module towards regions which may not be locally connected, both of which we hypothesized would yield better caricatures.

**Human-informed ground truth.** We collected heat maps corresponding to the locations of artifacts detectable by humans. First, we created a pool of challenging deepfake videos, as these are the most likely to yield non-trivial information about artifacts. From the DFDCp dataset [15], we selected 500 videos that are challenging for humans (see Supplement), and 500 videos that are challenging for the XceptionNet [40] detection model. We selected DFDCp because it provides the most variation among the deepfake datasets currently available: it includes low-light videos, profile and front-facing views of individuals, variations in resolution, quality, and actor movements. Next, we showed these deepfakes to a new set of participants (mean N=23 per video), who annotated areas of the videos that appeared distorted or manipulated (Figure 3). Participants were shown blocks of 100 3-second clips, and used a paint-brush interface to paint on videos regions that appeared unnatural (see Supplement). This resulted in over 11K annotations across 1000 videos. For each video clip, we aggregate all annotations and generate one 3D attention map by first applying an anisotropic Gaussian kernel of size (20, 20, 6) in  $x$ ,  $y$  and  $time$  dimensions, and then normalizing the map of each frame to sum to one. These attention maps will be made available on our project page upon publication.

**Module details and training.** The artifact attention module is based on the encoder-decoder architectural paradigm, and consists of an Xception-based encoder [11] and a 6-block Resnet-based decoder, where upsampling and convolutions are layered between each block (Figure 2). The encoder produces codes  $e$  that retain spatial information, and the decoder utilizes those compressed feature maps to generate output heatmaps. We use the human data to supervise the generation of these heatmaps directly. This happens through the sum of three losses:

the Pearson Correlation Coefficient, KL-Divergence, and L-1 loss. We confirmed that the Artifact Attention module achieves good performance at reproducing the ground truth maps: predicted maps had an average 0.745 Correlation Coefficient (CC) and a 0.452 KL divergence (KL) with the human-generated maps. In comparison, a simple 2D gaussian achieves 0.423 CC and 0.661 KL.

### 3.2. Classifier module

Our Classifier module (Figure 4) detects if the input is real or fake. This module receives feature maps generated by a global convolutional stem of three  $3 \times 3$  convolution layers with strides 2, 1 and 1. The layers use the Mish [34] activation function and implement Batch Normalization operations. A  $3 \times 3$  max pooling layer with stride 2 follows the stem, and a sequence of  $L$  Attention Blocks followed by a global average pooling and a sigmoid activation completes the Classifier Module. We define Attention Blocks as a Residual Block followed by a customized self-attention operation detailed in Figure 4b. We allow this module to supplement its self-attention with the human-guided attention information provided by the Artifact Attention Module, in order to increase attention to key parts of the input (details below). We analyzed Attention block sequence sizes of  $L = 18$  and  $L = 34$ : each alternative yields a different model version, referred to as CariNet18 and CariNet34. Cross entropy is used as the loss function. The output of the binary logit function is assigned to each frame as a detection score; we take the averaged score of the whole sequence as the prediction for the video clip.

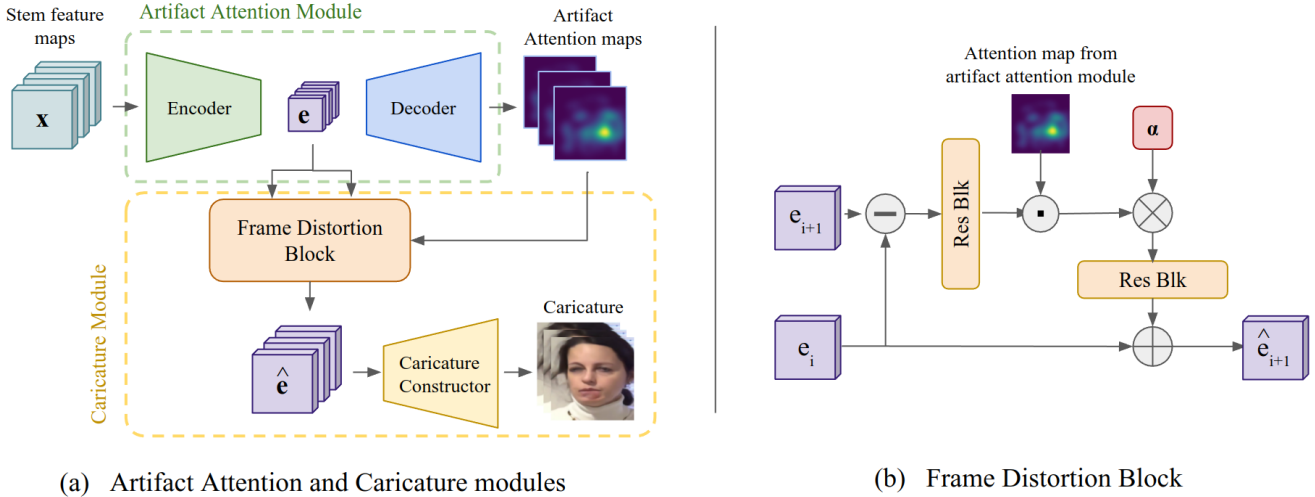
**Self-attention with artifact heatmaps.** We define our self-attention layers in a similar manner to prior self-attention work [54, 6], but we extended the traditional construction to incorporate modulation from the artifact attention heatmaps. Our self attention layer computes an affinity matrix between keys and queries, where the keys are re-weighted by the artifact attention map, putting more weight on the artifacts that are relevant to humans. Given a feature map  $\mathbf{x}_i$  over one frame, and an artifact attention map  $A$  over that frame, the module learns to generate an affinity matrix  $\mathbf{a}_i$ :

$$\mathbf{a}_i = \text{softmax}((\mathbf{W}_Q \mathbf{x}_i)^T (\mathbf{W}_K \mathbf{x}_i \odot \mathbf{A})). \quad (1)$$

The softmaxed key-query affinity tensor is then matrix-multiplied with the values  $V = W_V x_i$  to generate the output residual  $r$ . That residual is then scaled by  $\gamma$  and added to input  $x_i$  to yield the output feature map  $y_i$ :

$$\mathbf{y}_i = \gamma \mathbf{a}_i^T (\mathbf{W}_V \mathbf{x}_i) + \mathbf{x}_i. \quad (2)$$

$\mathbf{W}_Q, \mathbf{W}_K, \mathbf{W}_V$  are learned weight matrices of shape  $\mathbf{R}^{\bar{C} \times C}$ ,  $\mathbf{R}^{\bar{C} \times C}$  and  $\mathbf{R}^{C \times C}$  respectively, with  $\bar{C} = C/4$ .  $\gamma$  is a learnable scalar which controls the impact of the learned attention feature vis-a-vis the original feature maps  $x_i$ .



(a) Artifact Attention and Caricature modules

(b) Frame Distortion Block

Figure 2. **Our Artifact Attention and Caricature modules.** (a) The Artifact Attention and Caricature modules are intertwined: artifact attention operates with an encoder-decoder architecture to generate artifact heatmaps. Those heatmaps are supervised with the human heatmaps collected through our annotation interface. The Caricature module receives both the heatmaps and the internal codes  $e$ , distorts those codes according to the artifact attention heatmaps, and generates caricatures by reconstructing the video from the distorted codes. (b) Our frame distortion block computes the difference between codes  $e_i$  and  $e_{i+1}$ , re-weights it according to the artifact attention maps, and then amplifies it by a factor of  $\alpha$  before summing it back to  $e_i$  to generate distorted code  $\hat{e}_{i+1}$ .

### 3.3. Caricature Generation Module

Finally, the primary contribution of our framework is a novel module for creating Deepfake Caricatures, a visual indicator of video authenticity based on amplification of video artifacts. Figure 1 illustrates the distortion exhibited by our caricatures, but the effect is most compelling when viewed as a video (links to a gallery of caricatures can be found in the Supplement). Our Caricature Generation module leverages the encoder from the artifact attention module, distorts codes with a frame distortion block that operates over every pair of codes  $e_i$  and  $e_{i+1}$ , and uses a Caricature Constructor to create the final caricature (Figure 2). We instantiate the Caricature Constructor as a simple decoder with four blocks composed of 3x3 convolutions followed by nearest neighbor upsampling.

The caricature effect is achieved by amplifying the difference between the representations of consecutive frames, while guiding this amplification with the artifact attention maps generated by the artifact attention module. The guidance is introduced through element-wise multiplication between the tensor  $e_{diff} = ResBlk(e_{i+1} - e_i)$  and the artifact attention map of frame  $x_i$  (Figure 2b). This essentially results in a targeted distortion aiming at magnifying the artifacts highlighted by the heatmap.

The distorted code  $\hat{e}_i$  of frame  $x_i$  is computed as

$$\hat{e}_{i+1} = e_i + \alpha(e_{i+1} - e_i) \odot A, \quad (3)$$

where  $\alpha$  is a user-defined distortion factor that controls the strength of the resulting caricature.

### 3.4. Learning and Optimization

Training this framework is done in two phases. We first train the classification pipeline (Stem, Artifact Attention Module and Classifier) without the Caricature Module. We then freeze the classification pipeline and train the caricature module on a motion magnification task, before combining everything together to generate caricatures.

**Classification pipeline.** Our CariNets were separately trained on the DeepFake Detection Challenge (DFDCp) dataset, FaceForensics++, CelebDFv2 and DeeperForensics. For all datasets, we train on videos from the training set and evaluate on the validation or test set. We randomly sampled 32 frames from videos during training. Fake videos are over-represented in these datasets, so we over-sampled real videos during training to achieve real/fake balance. Our CariNets were optimized with Rectified Adam [30] with the LookAhead optimizer [55]. We use a batch size of 32 and an initial learning rate of 0.001. Cosine annealing learning rate scheduling was applied with half period of 100 epochs. We chose an early stopping strategy, stopping if validation accuracy stagnates in a 10 epoch window. We apply flipping (probability 0.5) and random cropping (224x224) augmentations. The full loss corresponds to the sum of the loss from the Classifier and Artifact Attention modules (described above).

**Caricature Module.** This module was trained following the motion magnification framework from [39]. We use their synthetic dataset, composed of triplets of frames  $(x_i, x_{i+1}, \hat{y}_{i+1})$  constructed to simulate motion magnifica-

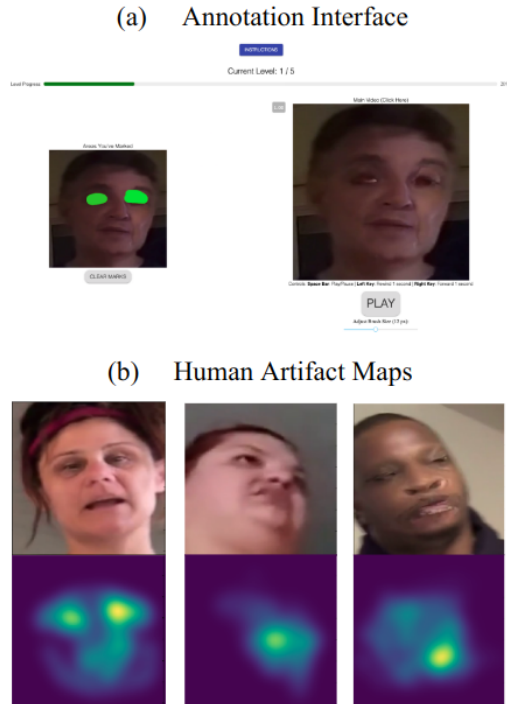


Figure 3. (a) Our annotation interface allows users to paint over particular artifacts or zones that appear fake. Our system tracks both the position and frame at which an annotation occurs. Users highlighted both large areas and more specific, semantically meaningful areas (e.g., eyebrows). (b) Examples of artifact maps created from averaging human annotations. Humans consistently highlighted areas with abnormal artifacts.

tion.  $x_i$  and  $x_{i+1}$  correspond to video frames at index  $i$  and  $i + 1$  (respectively), and  $\hat{y}_{i+1}$  corresponds to frame  $x_{i+1}$  with artificially magnified object displacements. During training, we compute encodings  $e_i$  and  $e_{i+1}$  with our frozen classification pipeline, and feed each pair to a Frame Distortion Block (2) that learns to generate  $\hat{e}_{i+1}$ , a distorted version of  $e_{i+1}$  where displacements are magnified. The caricature constructor then reconstructs an estimated magnified frame  $\bar{y}_{i+1}$ , which is compared to the ground truth magnified frame  $\hat{y}_{i+1}$  using a L-1 loss (no advantage found for more advanced losses). During this training period with the synthetic dataset, no attention maps are fed to the frame distortion block. After training, when generating a caricature, attention maps are used as a multiplicative modulation affecting the feature maps of the frame distortion block (as shown in Figure 2), which effectively turns magnifications on and off for different parts of the frame. This allows our module to function as a sort of *magnifying glass* over artifacts.

## 4. Model Experiments

The goal of our framework is to detect video forgeries, and provide a visual signal to human users in the form of Deepfake Caricatures. To assess the success of this approach, we first evaluate the model on deepfake detection accuracy, validating that it performs robust detection. We show that our model performs near the state of the art, and demonstrate that including the human annotations to supplement self-attention during training boosts model performance.

### 4.1. Evaluation Details

**Datasets.** We evaluate models on four benchmarks: *FaceForensics++ (FF++)* [40], which contains 1000 real videos and 4000 fake videos generated from four different facial manipulation methods [1, 46, 2, 45]. To ensure fair comparisons with [19] and others, we use the first 270 frames of each training video and the first 110 frames for each validation video.

*The Deepfake Detection Challenge Dataset (DFDCp)* [15]. We use the preview version of this dataset, which contains 3754 fakes and 1460 real videos generated using two different facial modification methods.

*Celeb-DF v2* [29]. This dataset contains high quality fake videos of celebrities generated from real Youtube videos. There are 590 original videos and 5639 corresponding deepfakes.

*DeeperForensics (DFo)* [29], which contains 10000 fake videos obtained by taking 1000 real videos from FF++, and swapping in faces of 100 new paid actors.

*FaceShifter (FShifter)* [25], which also consists of 10000 fake videos generated by manipulating the real videos from FF++.

Faces were standardized across datasets, such that each video was  $360 \times 360$  pixels, and showed a single face, with a minimum size of 50 pixels and a minimum margin of 100 pixels from the edge of the frame (see Supplement).

**Baseline comparisons.** We evaluate the accuracy of CariNet relative to several baselines from the literature: (1) *XceptionNet*, which was trained on the FaceForensics++ dataset [40]. (2) A *Frame-based ResNet18 and ResNet34* [21], which we use as a more general yet simple baseline for frame-based detection. (3) A *Clip-based ResNet* which uses 3D kernels inflated from ResNet18 pretrained on ImageNet [14] to learn over multiple frames at once [10, 20, 48], as well as a version pretrained on the Kinetics dataset [9]. We report results over our best ResNet: a 3DResnet-34 pretrained on Kinetics. (4) *Face X-ray*, which attends to the seams in face-swapping to make its predictions. We use existing performance values from [19] for the FF++ trained results, and evaluate an HRNet-W48 trained on synthetic blended images in conjunction with FF++ videos for our DFDCp results. (5) The *CNN-GRU*

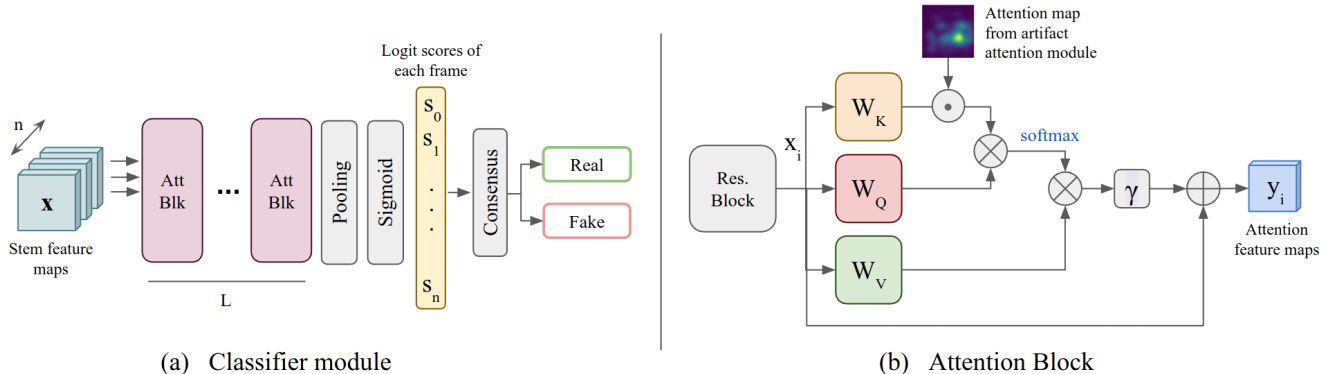


Figure 4. **The Classifier module and its attention blocks.** (a) our classifier takes the feature maps outputted by our convolutional stem, passes them through attention blocks modulated by human heatmaps, and computes logit scores for each frame before classifying the video. The consensus operation is instantiated as an average of the logits followed by thresholding to determine the output label. (b) Our attention block: a traditional residual block is followed by key, query and value matrices following the self-attention framework. The key-query product is modulated by our human heatmaps.  $\times$  represents matrix multiplication and  $\cdot$  represents element-wise multiplication.

Model	CelebDFv2	DFDCp	FShifter	DFo	Overall
3DResNet-34 (Kinetics)	72.1	64.9	72.2	74.5	70.9
Xception [40]	73.7	65.7	72.0	84.5	75.3
Face X-ray [26]	79.5	62.1	92.8	86.8	81.2
CNN-GRU [41]	69.8	63.7	80.8	74.1	73.4
Multi-task [36]	75.7	63.9	66.0	77.7	71.9
DSP-FWA [28]	69.5	64.5	65.5	50.2	63.1
Two-branch [31]	73.4	64.0	-	-	-
Multi-attention [56]	67.4	67.1	-	-	-
LipForensics [56]	82.4	70.0	<b>97.1</b>	97.6	86.8
CariNet18 (ours)	80.1	72.9	90.4	94.3	84.4
CariNet34 (ours)	<b>83.2</b>	<b>74.4</b>	93.9	<b>97.9</b>	<b>87.4</b>

Table 1. **Detection performance results on unseen datasets.** We report Video-level AUC (%) on four tested benchmarks. All models are pretrained on FF++ (all manipulations). In addition to this, our models (CariNet18 and CariNet34) leverage human artifact maps during learning. We only report the best performing ResNet baseline (3DResnet-34).

from [41], where we train a DenseNet-161 followed by a GRU on FF++ to evaluate on DFDCp, and report existing performance values for FF++. (6) *DSP-FWA*, a model that tries to detect face warping artifacts. We evaluate the publicly available pretrained model for FF++, and train a ResNet50 with the pyramidal setup introduced in [28] for DFDCp. (7) The *Multi-task* model from [36]. We report existing numbers from [19] and retrain using the publicly available implementation. (8) The *Two-branch* model from [31]. We report existing numbers for CelebDFv2 evaluation, and retrain on the rest. (9) The *Multi-attention* model from [56]. We report the values from the existing paper, and retrain following the setup in the paper on FF++ for DFDCp results.

## 4.2. Deepfake Detection Performance

**Generalization to unseen datasets.** At present, the performance of deepfake classifiers is assessed primarily based on their ability to generalize well to datasets built with dif-

ferent techniques from what the classifier was trained on. Thus, following the work of [19], we report our results as our model’s ability to train on one dataset and perform well on another. We train models on FF++ and evaluate their performance on CelebDFv2, DFDCp, FShifter and DFo. We note that the DFDCp videos used during evaluation were a different set than the DFDCp videos on which we collected human annotations, to ensure there was no data leak. Our CariNets show strong performance in this task, surpassing all previous alternatives in most benchmarks except for FaceShifter. We hypothesize that the attentional framework proposed allows CariNet to build more robust representation of artifact location and properties, focusing as needed on lips, eyes or other telling features. (Table 1).

**Cross-forgery detection** Several methods exist for creating deepfakes, and lead to different artifacts. In order to assess the quality of a detector, we must show good performance across deepfake-generation methods. We divided the FF++ dataset based on the deepfake-generation methods it

Method	Train on remaining				Avg
	DF	FS	F2F	NT	
Xception [40]	93.9	51.2	86.8	79.7	77.9
CNN-GRU [41]	97.6	47.6	85.8	86.6	79.4
Face X-ray [26]	99.5	93.2	94.5	92.5	94.9
LipForensics [19]	99.7	90.1	99.7	<b>99.1</b>	<b>99.5</b>
CariNet34 (ours)	<b>99.7</b>	<b>93.8</b>	<b>99.8</b>	97.5	99.0

Table 2. **Generalization to unseen manipulations.** Video-level AUC (%) on three of the forgery types of FaceForensics++ (Deepfakes (DF), Face2Face (F2F) and Neural Textures (NT)).

Method	Clean	Cont.	Noise	Blur	Pixel
Xception	99.8	98.6	53.8	60.2	74.2
CNN-GRU	99.9	98.8	47.9	71.5	86.5
Face X-ray	99.8	88.5	49.8	63.8	88.6
LipForensics	99.9	99.6	73.8	<b>96.1</b>	95.6
CariNet34	99.9	<b>99.8</b>	<b>74.5</b>	91.8	<b>96.3</b>

Table 3. **Generalization performance over unseen perturbations.** Video-level AUC (%) on FF++ over videos perturbed with 5 different modifications. We report averages across severity levels.

includes (Deepfake [1], FaceSwap [2], Face2Face [45], and NeuralTextures [45]). We trained the model on a subset of FF++ containing all four manipulations, and evaluated its performance on each method independently. In Table 2, we show performance against alternative models from the literature. Overall, our technique is on par with the best-performing model across generation methods.

**Robustness to unseen perturbations** Another key aspect of a forgery detector is the ability to maintain performance even when the input videos have degraded quality, causing new, unseen perturbations. To analyze CariNet’s behavior across types of perturbation, we test our model trained with FF++ on test videos from FF++ with 4 perturbations: Contrast, Gaussian Noise, Gaussian blur and Pixelation. We follow the framework of [19] and apply perturbations at 5 severity levels for our comparisons. We report average performance over the 5 severity levels in Table 3. We observe that our method outperforms previous approaches at most severity levels. We hypothesize that our human-guided attention framework might be of help in this setting, as humans are naturally capable of adapting to different lighting conditions, blurs, resolutions and other photometric modifications. This adaptability might be captured in the ground truth maps that guide the learning process of our Artifact Attention module.

### 4.3. Ablation studies

**Role of the Artifact Attention module.** We confirmed the contribution of adding human supervision via our Artifact Attention module by performing ablation studies across the different datasets under study. We observe performance decreases for CariNet18 following ablation in three dif-

ferent scenarios (Table 4): **(1)** removing our custom self-attention blocks (Figure 4) from the Classifier module, and replacing them with simple 3D residual blocks (each consisting of two 3x3x3 convolutions followed by batch normalization), **(2)** retraining self-attention blocks in the Classifier module, but removing the modulatory input from the Artifact Attention module (this yields regular attention blocks with no key modulation), **(3)** replacing the output of the Artifact Attention module with a fixed center bias, operationalized as a 2D gaussian kernel with mean  $\mu = (W/2, H/2)$  and standard deviation  $\sigma = (20, 20)$ . Overall, the complete model performed the best, demonstrating the effectiveness of incorporating self-attention modulated by human annotations into deepfake detection frameworks. Interestingly, using a fixed attention map degrades performance the most: this forces attention blocks to attend to parts of the input that don’t necessary contain valuable information related to the input’s manipulation.

## 5. Human Experiments

Next, in a user study, we test whether the Caricature technique is a successful decision aid for visually signalling that a video is fake. We find that Caricatures dramatically improve human detection of deepfakes.

**Brief Methods.** In a sample of 400 videos from the DFDCp (200 real, 200 fake), we compared the detectability of *standard* (i.e. unmodified) deepfakes with deepfakes *caricatures*. Videos were shown to human participants one at a time, and participants indicated if the video was real or fake. Crucially, we tested whether caricatures could improve deepfake detection even under challenging conditions such as very fast presentation times or low attentiveness. Videos were presented for 6 different durations: 300ms, 500ms, 1000ms, 3000ms, and 5000ms. Additionally, unbeknownst to participants, we embedded *engagement probes* in the experiment (5 trials per 100-trial HIT) in order to collect a measure of participant engagement. Engagement probes consisted of standard deepfakes with very large artifacts which were extremely easy to detect. We reasoned that highly-engaged participants would succeed on all of these trials, but medium to low-engagement participants would miss some proportion of them (see Supplement for detailed methods).

**Results.** In Figure 5 (top), we show the detectability of fake videos in each condition (green for caricature, orange for standard deepfake). For each video, we calculated the proportion of time it was correctly detected in a sample of 10 participants. Detectability was substantially higher for caricatures than standard deepfakes, averaged over all timepoints ( $F(2, 1630) = 17.12, p < 0.001$ ). The advantage for caricatures over standard deepfakes was significant at every timepoint tested (Bonferroni-corrected alpha of  $p=0.0083$ ). With as little as 300ms exposure, detection was better for

Model	DFDCp	FF++	CelebDFv2	DFo	Overall
CariNet18 w/o attention mechanism	70.92	93.73	73.9	84.56	80.78
CariNet18 w/o modulation from attention module	72.34	94.82	76.5	91.21	83.72
CariNet18 w/ fixed attention (Gaussian)	68.15	90.15	71.1	82.23	77.91
CariNet18 (ours)	<b>72.90</b>	<b>96.81</b>	<b>80.1</b>	<b>94.33</b>	<b>86.04</b>

Table 4. **Ablation study results.** We show how certain components of our approach affect video-level AUC (%). We remove the attention mechanism from the Classifier module, we retain the attention mechanism but prevent modulation from the human-informed Artifact Attention module, and we replace the human informed modulation with a fixed center bias. All modifications yield lower performance than our proposed network.

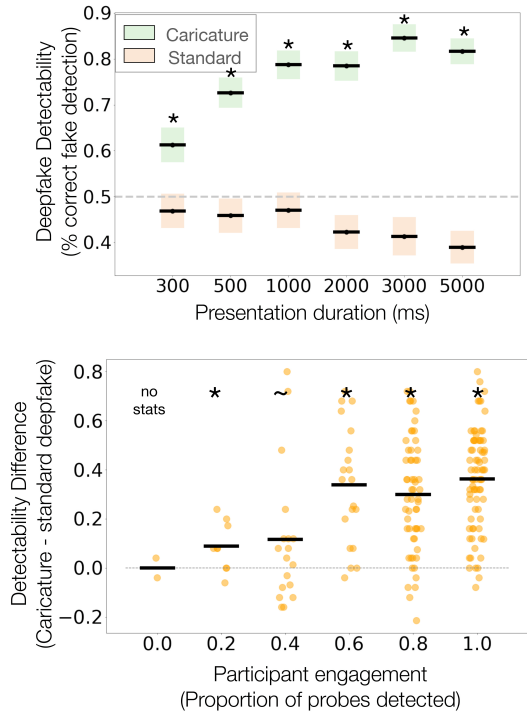


Figure 5. **Behavioral results showing the effect of caricatures on human deepfake detection.** Top Panel: Deepfake detectability by humans for standard (orange) and caricature (green) conditions. Colored boxes represent 95% confidence intervals, and stars indicate that the difference between conditions is significant. Bottom Panel: Improvement in deepfake detection with Caricatures, binned by participant engagement level.

caricatures by 14 percentage points, and this advantage increases to 43 percentage points for a 5 second exposure (significant interaction,  $F(10, 1630) = 8.88, p < 0.001$ ). Crucially, while standard deepfakes were detected no better than chance, caricatures boosted the likelihood of detection above 50% across all presentation times. Thus, caricatures increase the likelihood that a deepfake will be detected as fake, even when participants had less than a second of exposure. See Supplement for a full statistical reporting.

For artifact magnification to be a viable method of signaling deepfakes to humans, it should be effective even

when users are distracted or inattentive. In Figure 5 (bottom), we show how participant engagement impacts the effectiveness of the caricature technique. Participants were binned based on the number of engagement probes they correctly identified as fake, and the detection accuracy difference between caricatures and standard fakes was assessed for each bin. We find that caricatures yield higher detection at all but the lowest level of engagement (no stats were conducted for the lowest engagement bin, because it contained too few participants; all other comparisons were significant at  $p < 0.05$ , or marginal at  $p = 0.051$  in one case).

Overall, these behavioral results demonstrate that the caricature method is extremely effective at signalling to a human user that a video is fake. Not only does it allow for the correct detection of deepfakes from the first glimpse (as quickly as 300 ms), but it also protects people even when they are not being attentive and vigilant.

## 6. Conclusion and Discussion

This work takes a user-centered approach to deepfake detection models, and proposes a model whose focus is not just to detect video forgeries, but also alert the human user in an intuitive manner. Our CariNet shows excellent detection performance on four different datasets, and crucially, creates novel Deepfake Caricatures which allow for above-chance detection by human observers. Overall, this work establishes the importance of integrating computer vision and human factors solutions for deepfake mitigation, and additionally demonstrates the feasibility of improving human deepfake detection with machine assistance.

A constant challenge for such models is that deepfakes-generation methods are evolving at a vertiginous pace. Soon, diffusion models will be able to generate realistic video from text [42], potentially making deepfakes easier to create than ever. Our framework has certain advantages in this rapidly changing landscape. It leverages both human and machine intelligence, which may help it remain robust to new deepfakes, and it may be easier to update by adding new human attention maps as the technology evolves. More importantly, the insight that human detection can be improved by increasing the visibility of distortions has broad-ranging implications for the design of deepfake mitigation



software across platforms. The primary contribution of this work is a computer-vision supported method for highlighting artifacts and bringing them to the attention of the viewer.

As with any misinformation detection system, there is a risk that our network could be reverse engineered to produce higher quality deepfakes. However, a system which allows humans to directly detect if a video is doctored will empower them to assess for themselves whether to trust the video. Aggregated over millions of watchers, we believe that the benefits of such a system outweigh the risks.

## References

- [1] Deepfake. <https://github.com/deepfakes/faceswap>, 2020. 5, 7
- [2] Faceswap. <https://github.com/MarekKowalski/FaceSwap/>, 2020. 5, 7
- [3] Darius Afchar, Vincent Nozick, Junichi Yamagishi, and Isao Echizen. Mesonet: a compact facial video forgery detection network. In *2018 IEEE International Workshop on Information Forensics and Security (WIFS)*, pages 1–7. IEEE, 2018. 2
- [4] Jessica S Ancker, Alison Edwards, Sarah Nosal, Diane Hauser, Elizabeth Mauer, and Rainu Kaushal. Effects of workload, work complexity, and repeated alerts on alert fatigue in a clinical decision support system. *BMC medical informatics and decision making*, 17(1):1–9, 2017. 1, 2
- [5] Belhassen Bayar and Matthew C Stamm. A deep learning approach to universal image manipulation detection using a new convolutional layer. In *Proceedings of the 4th ACM Workshop on Information Hiding and Multimedia Security*, pages 5–10, 2016. 2
- [6] Irwan Bello, Barret Zoph, Ashish Vaswani, Jonathon Shlens, and Quoc V Le. Attention augmented convolutional networks. In *Proceedings of the IEEE/CVF international conference on computer vision*, pages 3286–3295, 2019. 3
- [7] Philip J Benson and David I Perrett. Perception and recognition of photographic quality facial caricatures: Implications for the recognition of natural images. *European Journal of Cognitive Psychology*, 3(1):105–135, 1991. 2
- [8] Aidan Boyd, Patrick Tinsley, Kevin Bowyer, and Adam Czajka. The value of ai guidance in human examination of synthetically-generated faces. *arXiv preprint arXiv:2208.10544*, 2022. 2
- [9] Joao Carreira, Eric Noland, Chloe Hillier, and Andrew Zisserman. A short note on the kinetics-700 human action dataset. *arXiv preprint arXiv:1907.06987*, 2019. 5
- [10] Joao Carreira and Andrew Zisserman. Quo vadis, action recognition? a new model and the kinetics dataset. In *proceedings of the IEEE Conference on Computer Vision and Pattern Recognition*, pages 6299–6308, 2017. 5
- [11] François Chollet. Xception: Deep learning with depthwise separable convolutions. In *Proceedings of the IEEE conference on computer vision and pattern recognition*, pages 1251–1258, 2017. 3
- [12] Umur Aybars Ciftci and Ilke Demir. Fakecatcher: Detection of synthetic portrait videos using biological signals. *arXiv preprint arXiv:1901.02212*, 2019. 2
- [13] Shuchisnigdha Deb and David Claudio. Alarm fatigue and its influence on staff performance. *IIE Transactions on Healthcare Systems Engineering*, 5(3):183–196, 2015. 1, 2
- [14] Jia Deng, Wei Dong, Richard Socher, Li-Jia Li, Kai Li, and Li Fei-Fei. Imagenet: A large-scale hierarchical image database. In *2009 IEEE conference on computer vision and pattern recognition*, pages 248–255. Ieee, 2009. 5
- [15] Brian Dolhansky, Russ Howes, Ben Pflaum, Nicole Baram, and Cristian Canton Ferrer. The deepfake detection challenge (dfd) preview dataset. *arXiv preprint arXiv:1910.08854*, 2019. 3, 5
- [16] Ricard Durall, Margret Keuper, Franz-Josef Pfreundt, and Janis Keuper. Unmasking deepfakes with simple features. *arXiv preprint arXiv:1911.00686*, 2019. 2
- [17] Matthew Groh, Ziv Epstein, Chaz Firestone, and Rosalind Picard. Deepfake detection by human crowds, machines, and machine-informed crowds. *Proceedings of the National Academy of Sciences*, 119(1), 2022. 1, 2
- [18] David Güera and Edward J Delp. Deepfake video detection using recurrent neural networks. In *2018 15th IEEE International Conference on Advanced Video and Signal Based Surveillance (AVSS)*, pages 1–6. IEEE, 2018. 2
- [19] Alexandros Haliassos, Konstantinos Vougioukas, Stavros Petridis, and Maja Pantic. Lips don’t lie: A generalisable and robust approach to face forgery detection. In *Proceedings of the IEEE/CVF Conference on Computer Vision and Pattern Recognition*, pages 5039–5049, 2021. 5, 6, 7
- [20] Kensho Hara, Hirokatsu Kataoka, and Yutaka Satoh. Can spatiotemporal 3d cnns retrace the history of 2d cnns and imagenet? In *The IEEE Conference on Computer Vision and Pattern Recognition (CVPR)*, 2018. 5
- [21] Kaiming He, Xiangyu Zhang, Shaoqing Ren, and Jian Sun. Deep residual learning for image recognition. In *Proceedings of the IEEE conference on computer vision and pattern recognition*, pages 770–778, 2016. 5
- [22] Mustafa I Hussain, Tera L Reynolds, and Kai Zheng. Medication safety alert fatigue may be reduced via interaction design and clinical role tailoring: a systematic review. *Journal of the American Medical Informatics Association*, 26(10):1141–1149, 2019. 1, 2
- [23] Haodong Li, Bin Li, Shunquan Tan, and Jiwu Huang. Identification of deep network generated images using disparities in color components. *Signal Processing*, 174:107616, 2020. 2
- [24] Jia Li, Tong Shen, Wei Zhang, Hui Ren, Dan Zeng, and Tao Mei. Zooming into face forensics: A pixel-level analysis. *arXiv preprint arXiv:1912.05790*, 2019. 2
- [25] Lingzhi Li, Jianmin Bao, Hao Yang, Dong Chen, and Fang Wen. Faceshifter: Towards high fidelity and occlusion aware face swapping. *arXiv preprint arXiv:1912.13457*, 2019. 5
- [26] Lingzhi Li, Jianmin Bao, Ting Zhang, Hao Yang, Dong Chen, Fang Wen, and Baining Guo. Face x-ray for more general face forgery detection. *arXiv preprint arXiv:1912.13458*, 2019. 2, 6, 7

- [27] Yuezun Li, Ming-Ching Chang, and Siwei Lyu. In ictu oculi: Exposing ai created fake videos by detecting eye blinking. In *2018 IEEE International workshop on information forensics and security (WIFS)*, pages 1–7. IEEE, 2018. [2](#)
- [28] Yuezun Li and Siwei Lyu. Exposing deepfake videos by detecting face warping artifacts, 2018. [2](#), [6](#)
- [29] Yuezun Li, Xin Yang, Pu Sun, Honggang Qi, and Siwei Lyu. Celeb-df: A new dataset for deepfake forensics. *arXiv preprint arXiv:1909.12962*, 2019. [5](#)
- [30] Liyuan Liu, Haoming Jiang, Pengcheng He, Weizhu Chen, Xiaodong Liu, Jianfeng Gao, and Jiawei Han. On the variance of the adaptive learning rate and beyond. *arXiv preprint arXiv:1908.03265*, 2019. [4](#)
- [31] Iacopo Masi, Aditya Killekar, Royston Marian Mascarenhas, Shenoy Pratik Gurudatt, and Wael AbdAlmageed. Two-branch recurrent network for isolating deepfakes in videos. In *European Conference on Computer Vision*, pages 667–684. Springer, 2020. [6](#)
- [32] Falko Matern, Christian Riess, and Marc Stamminger. Exploiting visual artifacts to expose deepfakes and face manipulations. In *2019 IEEE Winter Applications of Computer Vision Workshops (WACVW)*, pages 83–92. IEEE, 2019. [2](#)
- [33] Robert Mauro and Michael Kubovy. Caricature and face recognition. *Memory & Cognition*, 20(4):433–440, 1992. [2](#)
- [34] Diganta Misra. Mish: A self regularized non-monotonic neural activation function. *arXiv preprint arXiv:1908.08681*, 2019. [3](#)
- [35] Daniel Mas Montserrat, Hanxiang Hao, SK Yarlagadda, Sri-ram Baireddy, Ruiting Shao, János Horváth, Emily Bartusiak, Justin Yang, David Güera, Fengqing Zhu, et al. Deepfakes detection with automatic face weighting. *arXiv preprint arXiv:2004.12027*, 2020. [2](#)
- [36] Huy H Nguyen, Fuming Fang, Junichi Yamagishi, and Isao Echizen. Multi-task learning for detecting and segmenting manipulated facial images and videos. *arXiv preprint arXiv:1906.06876*, 2019. [6](#)
- [37] Huy H Nguyen, Junichi Yamagishi, and Isao Echizen. Capsule-forensics: Using capsule networks to detect forged images and videos. In *ICASSP 2019-2019 IEEE International Conference on Acoustics, Speech and Signal Processing (ICASSP)*, pages 2307–2311. IEEE, 2019. [2](#)
- [38] Sophie J Nightingale and Hany Farid. Ai-synthesized faces are indistinguishable from real faces and more trustworthy. *Proceedings of the National Academy of Sciences*, 119(8):e2120481119, 2022. [1](#)
- [39] Tae-Hyun Oh, Ronnachai Jaroensri, Changil Kim, Mohamed Elgharib, Fr'edo Durand, William T Freeman, and Wojciech Matusik. Learning-based video motion magnification. In *Proceedings of the European Conference on Computer Vision (ECCV)*, pages 633–648, 2018. [4](#)
- [40] Andreas Rossler, Davide Cozzolino, Luisa Verdoliva, Christian Riess, Justus Thies, and Matthias Nießner. Faceforensics++: Learning to detect manipulated facial images. In *Proceedings of the IEEE International Conference on Computer Vision*, pages 1–11, 2019. [3](#), [5](#), [6](#), [7](#)
- [41] Ekraam Sabir, Jiaxin Cheng, Ayush Jaiswal, Wael AbdAlmageed, Iacopo Masi, and Prem Natarajan. Recurrent convolutional strategies for face manipulation detection in videos. *Interfaces (GUI)*, 3:1. [2](#), [6](#), [7](#)
- [42] Uriel Singer, Adam Polyak, Thomas Hayes, Xi Yin, Jie An, Songyang Zhang, Qiyuan Hu, Harry Yang, Oron Ashual, Oran Gafni, et al. Make-a-video: Text-to-video generation without text-video data. *arXiv preprint arXiv:2209.14792*, 2022. [8](#)
- [43] Pawan Sinha, Benjamin Balas, Yuri Ostrovsky, and Richard Russell. Face recognition by humans: Nineteen results all computer vision researchers should know about. *Proceedings of the IEEE*, 94(11):1948–1962, 2006. [2](#)
- [44] Joel Stehouwer, Hao Dang, Feng Liu, Xiaoming Liu, and Anil Jain. On the detection of digital face manipulation. *arXiv preprint arXiv:1910.01717*, 2019. [2](#)
- [45] Justus Thies, Michael Zollhöfer, and Matthias Nießner. Deferred neural rendering: Image synthesis using neural textures. *ACM Transactions on Graphics (TOG)*, 38(4):1–12, 2019. [5](#), [7](#)
- [46] Justus Thies, Michael Zollhofer, Marc Stamminger, Christian Theobalt, and Matthias Nießner. Face2face: Real-time face capture and reenactment of rgb videos. In *Proceedings of the IEEE conference on computer vision and pattern recognition*, pages 2387–2395, 2016. [5](#)
- [47] Ruben Tolosana, Sergio Romero-Tapiador, Julian Fierrez, and Ruben Vera-Rodriguez. Deepfakes evolution: Analysis of facial regions and fake detection performance, 2020. [2](#)
- [48] Du Tran, Heng Wang, Lorenzo Torresani, Jamie Ray, Yann LeCun, and Manohar Paluri. A closer look at spatiotemporal convolutions for action recognition. In *Proceedings of the IEEE conference on Computer Vision and Pattern Recognition*, pages 6450–6459, 2018. [5](#)
- [49] Philipp Tschandl, Christoph Rinner, Zoe Apalla, Giuseppe Argenziano, Noel Codella, Allan Halpern, Monika Janda, Aimilios Lallas, Caterina Longo, Josep Malvehy, John Paoli, Susana Puig, Cliff Rosendahl, H. Peter Soyer, Iris Zalaudek, and Harald Kittler. Human–computer collaboration for skin cancer recognition. *Nature Medicine*, 26(8):1229–1234, Aug 2020. [1](#), [2](#)
- [50] Barbara Tversky and Daphna Baratz. Memory for faces: Are caricatures better than photographs? *Memory & cognition*, 13(1):45–49, 1985. [2](#)
- [51] Michelle Vaccaro and Jim Waldo. The effects of mixing machine learning and human judgment: Collaboration between humans and machines does not necessarily lead to better outcomes. *Queue*, 17(4):19–40, 2019. [2](#)
- [52] Danqi Xing, Jun Yang, Jing Jin, and Xiangyu Luo. Potential of plant identification apps in urban forestry studies in china: comparison of recognition accuracy and user experience of five apps. *Journal of Forestry Research*, 32(5):1889–1897, Oct 2021. [1](#), [2](#)
- [53] Xin Yang, Yuezun Li, and Siwei Lyu. Exposing deep fakes using inconsistent head poses. In *ICASSP 2019-2019 IEEE International Conference on Acoustics, Speech and Signal Processing (ICASSP)*, pages 8261–8265. IEEE, 2019. [2](#)
- [54] Han Zhang, Ian Goodfellow, Dimitris Metaxas, and Augustus Odena. Self-attention generative adversarial networks. *arXiv preprint arXiv:1805.08318*, 2018. [3](#)

- [55] Michael R Zhang, James Lucas, Geoffrey Hinton, and Jimmy Ba. Lookahead optimizer: k steps forward, 1 step back. *arXiv preprint arXiv:1907.08610*, 2019. 4
- [56] Hanqing Zhao, Wenbo Zhou, Dongdong Chen, Tianyi Wei, Weiming Zhang, and Nenghai Yu. Multi-attentional deep-fake detection. In *Proceedings of the IEEE/CVF Conference on Computer Vision and Pattern Recognition*, pages 2185–2194, 2021. 6